Mineralogical Magazine (2020), **84**, 275–282
doi:10.1180/mgm.2020.15

CAMBRIDGE UNIVERSITY PRESS

Article

Redefinition of coquimbite, $AlFe_3^{3+}(SO_4)_6(H_2O)_{12}\cdot 6H_2O$

Daniela Mauro[1]*, Cristian Biagioni[1], Marco Pasero[1], Henrik Skogby[2] and Federica Zaccarini[3]

[1]Dipartimento di Scienze della Terra, Università di Pisa, Via Santa Maria 53, 56126 Pisa, Italy; [2]Department of Geosciences, Swedish Museum of Natural History, Box 50007, SE-10405 Stockholm, Sweden; and [3]Department of Applied Geological Sciences and Geophysics, University of Leoben, Peter Tunner Str. 5, A-8700 Leoben, Austria

Abstract

Coquimbite, $AlFe_3^{3+}(SO_4)_6(H_2O)_{12}\cdot 6H_2O$, was considered as a pure Fe^{3+} hydrated sulfate. However, previous mineralogical studies pointed out the occurrence of essential Al, occupying a distinct site in the crystal structure of this mineral. Through the critical re-examination of the available literature and new crystal-chemical data collected on a specimen from the Monte Arsiccio mine, Apuan Alps, Tuscany, Italy, the chemical formula of coquimbite has been revised, taking into account the occurrence of Al. Coquimbite has a homeotypic relationship with paracoquimbite, $Fe_4(SO_4)_6(H_2O)_{12}\cdot 6H_2O$; both mineral species belong to the coquimbite group. On the contrary, aluminocoquimbite, $Al_2Fe_2(SO_4)_6(H_2O)_{12}\cdot 6H_2O$, has a different topology and does not belong to that group.

Keywords: coquimbite, iron, aluminium, sulfate, paracoquimbite, aluminocoquimbite, coquimbite group

(Received 10 January 2020; accepted 25 February 2020; Accepted Manuscript published online: 2 March 2020; Associate Editor: František Laufek)

Introduction

Ferric iron sulfates are important minerals typically formed through the weathering of pyrite (e.g. Jambor *et al.*, 2000). According to the International Mineralogical Association (IMA) List of Minerals (accessed in May 2019; Pasero, 2019), the system Fe_2O_3–SO_3–H_2O consists of 16 mineral species (Table 1). Among them, five phases share the same formula $Fe_2(SO_4)_3\cdot nH_2O$, where $n = 5$ (lausenite), 7 (kornelite), 9 (coquimbite and paracoquimbite) and 11 (quenstedtite). However, the inclusion of coquimbite into the Fe_2O_3–SO_3–H_2O ternary system is doubtful, owing to the uncertainty in its definition. Indeed, as pointed out by previous structural studies (i.e. Fang and Robinson, 1970; Giacovazzo *et al.*, 1970; Majzlan *et al.*, 2006 and 2010; Demartin *et al.*, 2010a; Yang and Giester, 2018), aluminium seems to be an essential component in the crystal structure of coquimbite. Notwithstanding the unequivocal results of some of these studies, coquimbite was still reported as an Al-free ferric iron sulfate.

In order to define the actual chemical formula of coquimbite, a critical examination of the available literature was performed. None of the available crystal-chemical works gave a full set of data (high quality single-crystal X-ray diffraction or electron microprobe data collected in wavelength dispersive mode). Consequently, the aim of this paper is two-fold: discussing the previous mineralogical studies on coquimbite and related minerals, and providing a new set of data collected on specimens from a new finding of coquimbite. These data fully agree with the previous results and supported the proposal for the redefinition of coquimbite as an aluminium-ferric iron sulfate. In addition, the coquimbite group is proposed, in accord with the guidelines on group nomenclature (Mills *et al.*, 2009). The proposal has been accepted by the IMA-CNMNC (proposal 19-F, Miyawaki *et al.*, 2019).

*Author for correspondence: Daniela Mauro, Email: daniela.mauro@dst.unipi.it
Cite this article: Mauro D., Biagioni C., Pasero M., Skogby H. and Zaccarini F. (2020) Redefinition of coquimbite, $AlFe_3^{3+}(SO_4)_6(H_2O)_{12}\cdot 6H_2O$. *Mineralogical Magazine* **84**, 275–282. https://doi.org/10.1180/mgm.2020.15

Coquimbite and related minerals: a review

From the type description of coquimbite to the first X-ray diffraction studies

Coquimbite was described as a new mineral species from Coquimbo, Chile by Rose (1833), who called it "*neutrales schwefelsaures Eisenoxyd mit Krystallisationswasser*". According to the type description, this mineral was found "*in der Provinz Coquimbo* […] *und zwar im district Copiapo*" (Rose, 1833). Chemical data reported in the type description indicate only minor Al_2O_3 (0.92 wt.%). The name 'coquimbite', after the type locality, was first introduced by Breithaupt (1841).

Arzruni (1879) gave additional information about the occurrence of coquimbite and discussed its morphology and chemistry. In that paper, the results of the chemical analyses performed by Bamberger were presented, indicating that the formula of coquimbite should be written as '(¼ Al_2 + ¾ $Fe_2)(SO_4)_3$ + 9 H_2O'. By recalculating this formula on the basis of six (SO_4) groups per formula unit, it becomes $AlFe_3(SO_4)_6\cdot 18H_2O$.

New chemical data were given by Linck (1889). No Al_2O_3 was reported, in contrast to the previous data given by Arzruni (1879). Subsequent data given by Collins (1923), who described this mineral from the Concepcion mine, Spain, found 2.25 wt.% Al_2O_3, also confirmed by Lausen (1928), who pointed out the high Al content (6.93 wt.% Al_2O_3) occurring in coquimbite from the United Verde mine, Arizona, USA. On the contrary, Scharizer (1927) and Bandy (1938) gave Al-free chemical data for coquimbite, in agreement with Linck (1889).

It is worth noting that Bandy (1938) gave similar data for both coquimbite and paracoquimbite.

Table 1. Mineral species in the system Fe_2O_3–SO_3–H_2O.

Mineral	Chemical formula	*a* (Å)	*b* (Å)	*c* (Å)	α (°)	β (°)	γ (°)	S.g.	Reference
Amarantite	$Fe_2O(SO_4)_2{\cdot}7H_2O$	8.98	11.68	6.70	95.6	90.4	97.2	$P\bar{1}$	Susse (1968)
Butlerite	$Fe(SO_4)(OH){\cdot}2H_2O$	6.50	7.37	5.84	90	108.4	90	$P2_1/m$	Fanfani *et al.* (1971)
Coquimbite	$Fe_2(SO_4)_3{\cdot}9H_2O$	10.93	10.93	17.07	90	90	120	$P\bar{3}1c$	This work
Ferricopiapite	$Fe_{0.67}Fe_4(SO_4)_6(OH)_2{\cdot}20H_2O$	7.39	18.38	7.34	93.9	102.2	98.9	$P\bar{1}$	Majzlan and Kiefer (2006)
Fibroferrite	$Fe(SO_4)(OH){\cdot}5H_2O$	24.20	24.20	7.65	90	90	120	$R3$	Ventruti *et al.* (2016)
Hohmannite	$Fe_2O(SO_4)_2{\cdot}8H_2O$	9.14	10.93	7.22	90.5	90.6	107.4	$P\bar{1}$	Ventruti *et al.* (2015)
Hydroniumjarosite	$(H_3O)Fe_3(SO_4)_2(OH)_6$	7.34	7.34	17.05	90	90	120	$R\bar{3}m$	Plášil *et al.* (2014)
Kornelite	$Fe_2(SO_4)_3{\cdot}7H_2O$	14.30	20.12	5.42	90	96.8	90	$P2_1/n$	Robinson and Fang (1973)
Lausenite	$Fe_2(SO_4)_3{\cdot}5H_2O$	10.68	11.05	5.55	90	98.9	90	$P2_1/m$	Majzlan *et al.* (2005)
Metahohmannite	$Fe_2O(SO_4)_2{\cdot}4H_2O$	7.35	9.77	7.15	91.7	98.5	86.4	$P\bar{1}$	Scordari *et al.* (2004)
Parabutlerite	$Fe(SO_4)(OH){\cdot}2H_2O$	36.98	20.06	7.23	90	90	90	$P2_12_12_1$	Majzlan *et al.* (2018)
Paracoquimbite	$Fe_2(SO_4)_3{\cdot}9H_2O$	10.96	10.96	51.47	90	90	120	$R\bar{3}$	Yang and Giester (2018)
Quenstedtite	$Fe_2(SO_4)_3{\cdot}11H_2O$	6.18	23.60	6.54	94.2	101.7	96.3	$P\bar{1}$	Thomas *et al.* (1974)
Rhomboclase	$(H_5O_2)Fe(SO_4)_2{\cdot}2H_2O$	9.69	18.20	5.42	90	90	90	$Pnma$	Peterson *et al.* (2009)
Schwertmannite	$Fe_{16}O_{16}(OH)_{9.6}(SO_4)_{3.2}{\cdot}10H_2O$	10.8	6.0	10.5	90	93	90	$P1$	Fernandez-Martinez *et al.* (2010)
Volaschioite	$Fe_4(SO_4)O_2(OH)_6{\cdot}2H_2O$	16.07	3.06	10.93	90	93.8	90	$C2/m$	Biagioni *et al.* (2011)

S.g. – space group; chemical formulae after the official IMA List of Minerals (Pasero, 2019).

The latter phase was described by Ungemach (1933, 1935) during the re-examination of the specimens studied by Linck (1889), stored in the mineralogical collection of the University of Strasbourg, France, as a dimorph of coquimbite. The distinction between these two minerals was based upon some morphological and physical features as well as upon X-ray data collected through the Laue method. X-ray diffraction proved that coquimbite is trigonal with a primitive lattice, whereas paracoquimbite has a rhombohedral lattice. According to the data given by Ungemach (1935), the chemistry of these two minerals is very similar and both display only trace amounts of Al_2O_3.

Owing to the uncertain Al content, the ideal formula $Fe_2(SO_4)_3{\cdot}9H_2O$ was used throughout for both coquimbite and paracoquimbite (e.g. Palache *et al.*, 1951). This is the same chemical formula that was reported in the official IMA List of Minerals (Pasero, 2019), ignoring the results of the crystallographic studies carried out in the 1970s.

Fig. 1. Pseudo-hexagonal crystals of coquimbite, up to 1.5 cm in size. Monte Arsiccio mine, Apuan Alps, Italy (specimen in private collection).

Structural studies and the role of Al in coquimbite

Cesbron (1964) determined the space group of coquimbite as $P\bar{3}1c$, using a sample from Tierra Amarilla, Chile (Musèum National d'Histoire Naturelle, Paris sample MHNN 13373).

The crystal structure of coquimbite was first solved through single-crystal X-ray diffraction data by Fang and Robinson (1970) and Giacovazzo *et al.* (1970). The former, using a sample from Tierra Amarilla stored in the National Museum of Natural History (Smithsonian Institution) in Washington DC, USA (catalogue number 12548), found the presence of an Al-centred octahedron with the cation at (0, 0, 0) (site 2*b*), with site occupancy ($Al_{0.90}Fe_{0.10}$). The structural data were confirmed by wet chemical analysis. Giacovazzo *et al.* (1970) achieved similar results studying a sample from the Dexter mine, Utah, USA, obtaining an occupancy for the octahedral 2*b* site of ($Al_{0.63}Fe_{0.37}$). Aluminium and iron were determined chemically through colorimetric methods.

The crystal structure of the related mineral paracoquimbite was solved by Robinson and Fang (1971) using a sample from Chuquicamata, Chile stored in the National Museum of Natural History (Smithsonian Institution, USA; catalogue number 115161). As pointed out by the authors, no Al_2O_3 was detected, contrasting with the extensive Al-to-Fe substitution observed in coquimbite. The relationship between paracoquimbite and coquimbite was later discussed by Fang and Robinson (1974).

Majzlan *et al.* (2006) refined the crystal structure of coquimbite from the Richmond mine, Iron Mountain, California, USA, using synchrotron powder X-ray diffraction data, further confirming the occurrence of an Al-dominant octahedron in the crystal structure of coquimbite, with site occupancy ($Al_{0.91}Fe_{0.09}$). Minor Al was found at the Fe(3) site at (⅔, ⅓, *z*), with site occupancy ($Fe_{0.93}Al_{0.07}$). Inductively-coupled plasma optical emission spectroscopy confirmed the occurrence of Al in coquimbite.

Demartin *et al.* (2010a) studied three samples of coquimbite from Vulcano, Italy; Alcaparrosa, Chile; and from the Dexter No. 7 mine, Utah, USA. In all cases, the 2*b* site was occupied by Al, with only a partial replacement by Fe^{3+} (i.e. $Al_{0.76}Fe_{0.24}$) in the Chilean specimen. Structural data were supported through energy-dispersive spectroscopy (EDS) chemical analyses. A fourth sample, from Vulcano, was particularly enriched in Al and it was described as the new mineral species aluminocoquimbite (Demartin *et al.*, 2010a,b). Demartin *et al.* (2010a) were the first to locate the hydrogen atoms in the crystal structure of coquimbite. Their data were confirmed through neutron diffraction by Majzlan *et al.* (2010) using a sample from the Dexter No. 7 mine, Utah,

https://doi.org/10.1180/mgm.2020.15 Published online by Cambridge University Press

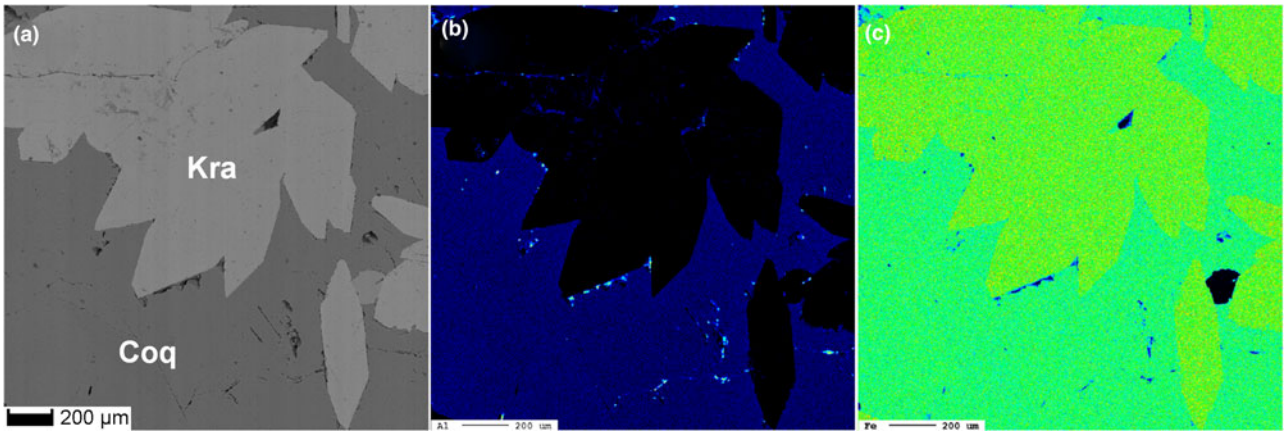

Fig. 2. Back-scattered electron image (*a*) and X-ray maps for Al (*b*) and Fe (*c*) of coquimbite (Coq) associated with krausite (Kra) from Monte Arsiccio.

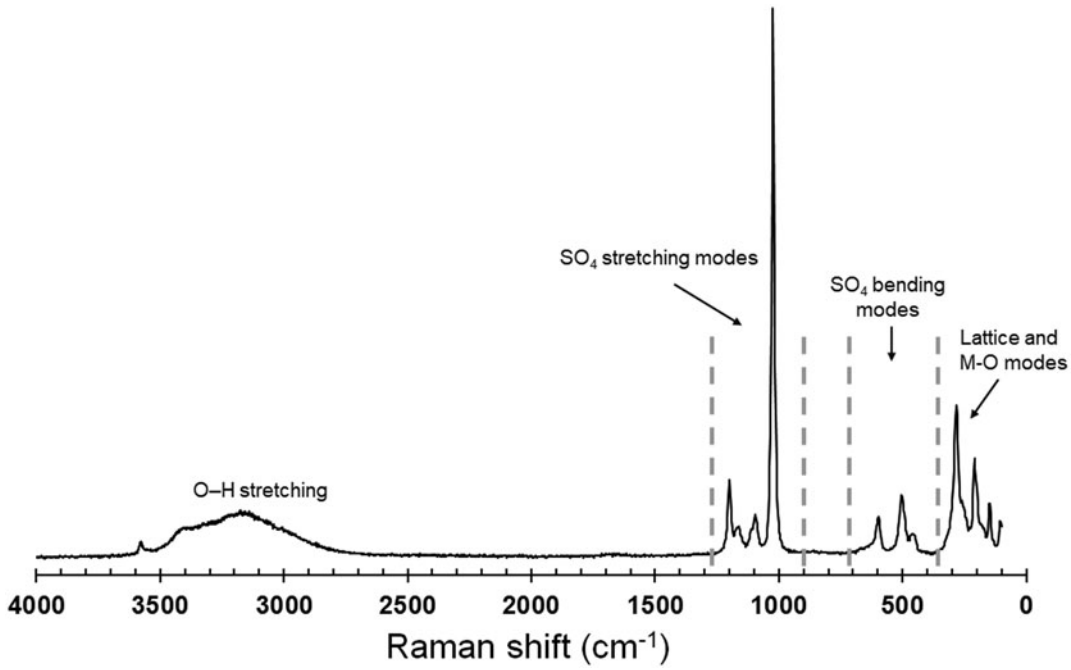

Fig. 3. Raman spectrum of coquimbite from Monte Arsiccio and band interpretation.

USA. This study confirmed, through neutron and X-ray diffraction, that the 2*b* site is occupied dominantly by Al. Meanwhile, a new refinement performed by Ackermann *et al.* (2009) on the synthetic analogue of paracoquimbite confirmed the previous results of Robinson and Fang (1971), indicating that all octahedral sites in this phase are occupied by Fe^{3+} only.

Frost *et al.* (2014) discussed the infrared and Raman spectra of coquimbite, using a specimen from the Javier Ortega mine, Peru. Chemical analysis, performed using EDS, gave the formula $(Fe_{1.37}Al_{0.63})(SO_4)_3{\cdot}9H_2O$, corresponding to $Al_{1.26}Fe_{2.74}(SO_4)_6{\cdot}18H_2O$ ($Z = 2$).

Finally, Yang and Giester (2018) re-examined the crystal structures of both coquimbite and paracoquimbite, giving the location of hydrogen atoms in the latter species. For the first time, they proposed the correct formula $AlFe_3(SO_4)_6{\cdot}18H_2O$ ($Z = 2$) for coquimbite, suggesting that a revision of its chemical formula is necessary. Unfortunately, their structural data, indicating the site occupancy ($Al_{0.66}Fe_{0.34}$) for the 2*b* site, were not supported by chemical data, which indicate the occurrence of only negligible Al. Paracoquimbite, on the contrary, was confirmed to be a pure Fe^{3+}-sulfate.

Coquimbite from the Monte Arsiccio mine, Apuan Alps, Italy

The specimen of coquimbite studied was collected in the Monte Arsiccio mine, Apuan Alps, Tuscany, Italy (43°58'0″N, 10° 16'59″E), where a complex sulfate assemblage has been recently discovered (e.g. Biagioni *et al.*, 2019). Coquimbite occurs as purple pseudo-hexagonal crystals (Fig. 1), up to 3 cm across, associated with halotrichite, römerite, melanterite, alunogen, krausite and rarely khademite. The identification of this specimen was confirmed through the collection of a powder X-ray diffraction pattern using a 114.6 mm Gandolfi camera and Ni-filtered Cu*K*α radiation.

https://doi.org/10.1180/mgm.2020.15 Published online by Cambridge University Press

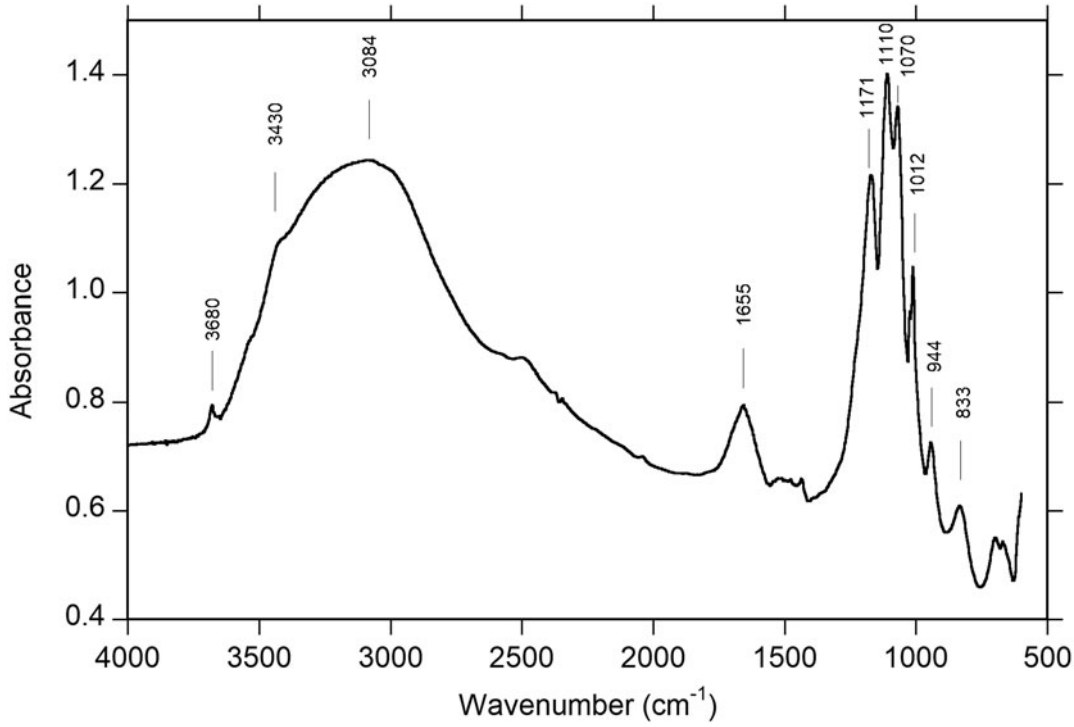

Fig. 4. Fourier-transfer infrared (FTIR) spectrum of coquimbite from Monte Arsiccio.

Chemistry

Quantitative chemical data were collected using a Superprobe JEOL JXA 8200 electron microprobe (wavelength-dispersive spectrosopy mode, 15 kV, 10 nA and 10 µm beam diameter) at the Eugen F. Stumpfl laboratory, Leoben University, Austria. Standards (element, emission line) were: hematite (Fe*K*α); kaersutite (Al*K*α); and baryte (S*K*α). The average of 20 spot analyses gave (in wt.%): SO_3 42.88(45), Al_2O_3 4.38(7), Fe_2O_3 22.28(38), $H_2O_{(calc)}$ 29.10, total 98.64. The H_2O content was calculated on the basis of structural data, which confirmed the occurrence of 18 H_2O groups. The empirical formula, based on 42 oxygen atoms, is $Al_{0.96}Fe_{3.11}S_{5.97}O_{24}\cdot 18H_2O$. X-ray maps, collected using the same analytical conditions reported for electron microprobe data, show the homogeneous distribution of Al and Fe within the grain studied (Fig. 2), which was associated closely with euhedral krausite, ideally $KFe(SO_4)_2\cdot H_2O$.

Micro-Raman and infrared spectroscopies

Micro-Raman spectrum of coquimbite (Fig. 3) was collected on an unpolished sample using a Horiba Jobin-Yvon XploRA Plus apparatus, with a 10× objective lens and the 532 nm line of a solid-state laser attenuated to 10% (i.e. 2.5 mW) in order to minimise sample damage. The spectrum was collected through multiple acquisitions with single counting times of 60 s. Back-scattered radiation was analysed with a 1200 grooves per cm grating monochromator. The spectral features fully agree with the results of Frost *et al.* (2014). The strongest band occurs at 1024 cm^{-1} and is due to the ν_1 mode of the SO_4 groups. Three low intensity bands at 1199, 1163, and 1096 cm^{-1} can be assigned to the antisymmetrical stretching mode ν_3 of SO_4 groups. The bending mode of SO_4 groups are represented by bands at 507, 456 (ν_2 mode) and 597 cm^{-1} (ν_4 mode). Lattice, Fe-O and Al-O vibration modes are observed at 311, 283, 255, 209, 181 and 150 cm^{-1}. Broad and intense Raman bands are observed in the region between 3600–2900 cm^{-1}. These Raman bands at 3577, 3423, 3179 and 2997 cm^{-1}, can be attributed to the stretching vibration mode of O–H bonds.

Table 2. Summary of crystal data and parameters describing data collection and refinement for coquimbite.

Crystal data	
Structural formula	$(Al_{0.94}Fe_{0.06})Fe_3(SO_4)_6(H_2O)_{12}\cdot 6H_2O$
Crystal size (mm^3)	0.15 × 0.12 × 0.10
Crystal system, space group	Trigonal, $P\bar{3}1c$
Temperature (K)	293
a, *c* (Å)	10.9318(12), 17.069(2)
V ($Å^3$)	1766.6(4)
Z	2
µ (mm^{-1})	1.75
Data collection and refinement	
Instrument	Bruker Smart Breeze
Radiation, wavelength (Å)	Mo*K*α, λ = 0.71073
T_{min}, T_{max}	0.904, 0.932
Maximum observed 2θ (°)	55.00
Measured reflections	16,979
Unique reflections	1341
Reflections $F_o > 4\sigma(F_o)$	1307
R_{int} after absorption correction	0.0185
*R*σ	0.0092
Range of *h*, *k*, *l*	$-14 \le h \le 14$, $-14 \le k \le 13$, $-22 \le l \le 21$
Refinement	
R [F_o>4 σ F_o]	0.0219
R (all data)	0.0224
wR (on F_o^2)	0.0664
Gof	1.083
Number of least-squares parameters	110
Maximum and minimum residual peak ($e^-/Å^3$)	0.82 [at 2.87 Å from H(21)], −0.33 [at 0.68 Å from S]

Weighting scheme is defined as $w = 1/[\sigma^2(F_o^2) + (aP)^2 + bP]$, where $P = [2F_c^2 + \mathrm{Max}(F_o^2, 0)]/3$. The *a* and *b* values are 0.0293 and 2.3592, respectively.

https://doi.org/10.1180/mgm.2020.15 Published online by Cambridge University Press

Table 3. Sites, Wyckoff positions, site occupancy factors (s.o.f.), fractional atom coordinates and isotropic (*) or equivalent isotropic displacement parameters in coquimbite.

Site	Wyckoff position	s.o.f.	*x/a*	*y/b*	*z/c*	U_{eq} (Å^2)
Al	2*b*	$Al_{0.946(7)}Fe_{0.054(7)}$	0	0	0	0.0132(4)
Fe(1)	2*c*	$Fe_{1.00}$	⅓	⅔	¼	0.01170(16)
Fe(2)	4*f*	$Fe_{1.00}$	⅔	⅓	0.00259(3)	0.01726(15)
S	12*i*	$S_{1\cdot00}$	0.24467(4)	0.41495(4)	0.12299(2)	0.01426(15)
O(1)	12*i*	$O_{1\cdot00}$	0.31822(14)	0.34515(14)	0.09097(9)	0.0239(3)
O(2)	12*i*	$O_{1\cdot00}$	0.10817(14)	0.31079(14)	0.15501(8)	0.0226(3)
O(3)	12*i*	$O_{1\cdot00}$	0.21965(15)	0.49421(14)	0.05998(8)	0.0218(3)
O(4)	12*i*	$O_{1\cdot00}$	0.33578(13)	0.51613(13)	0.18445(7)	0.0176(3)
Ow(1)	12*i*	$O_{1\cdot00}$	0.16494(15)	0.07034(14)	0.06168(9)	0.0224(3)
Ow(2)	12*i*	$O_{1\cdot00}$	0.44914(18)	0.11626(18)	0.20991(10)	0.0320(4)
Ow(3)	12*i*	$O_{1\cdot00}$	0.57193(18)	0.16215(17)	0.07119(9)	0.0298(4)
H(11)	12*i*	$H_{1\cdot00}$	0.187(4)	0.015(4)	0.0898(19)	0.070(11)*
H(12)	12*i*	$H_{1\cdot00}$	0.224(3)	0.165(2)	0.073(2)	0.058(10)*
H(21)	12*i*	$H_{1\cdot00}$	0.366(2)	0.033(2)	0.2069(19)	0.044(8)*
H(22)	12*i*	$H_{0.47(4)}$	0.510(6)	0.104(7)	0.242(4)	0.057(15)*
H(23)	12*i*	$H_{0.53(4)}$	0.443(6)	0.191(5)	0.229(4)	0.057(15)*
H(31)	12*i*	$H_{1\cdot00}$	0.599(4)	0.096(3)	0.074(2)	0.060(10)*
H(32)	12*i*	$H_{1\cdot00}$	0.529(4)	0.155(4)	0.1190(14)	0.069(11)*

Unpolarised Fourier transfer infrared absorption spectra of coquimbite (Fig. 4) were measured on powdered sample material mixed with KCl and pressed to a pellet. A Bruker Vertex spectrometer equipped with a Globar source, a KBr beam-splitter, an MCT detector, and a Hyperion 2000 microscope was used to acquire spectra in the wavenumber range 4000–600 cm^{-1} with a resolution of 4 cm^{-1}. The spectrum shows strong similarities with that of Frost *et al.* (2014), with a strong absorption band with some shoulder features in the 3700–2900 cm^{-1} range caused by O–H stretching motions, a distinctive band at 1655 cm^{-1} due to the H_2O bending mode, and a number of more narrow bands in the range 1200–1000 cm^{-1} that can be attributed to antisymmetric and symmetric stretching modes of SO_4 groups.

Single-crystal X-ray diffraction and crystal-structure refinement

X-ray diffraction intensity data were collected using a Bruker Smart Breeze diffractometer (50 kV and 30 mA) equipped with a Photon II CCD detector. Graphite monochromatised Mo*K*α radiation was used. The detector-to-crystal working distance was 50 mm. A total of 654 frames were collected using φ and ω scan modes with an exposure time of 10 s per frame. The data were integrated and corrected for Lorentz-polarisation, background effects and absorption, using the *Apex*3 software package (Bruker AXS Inc., 2016), resulting in a set of 16,979 reflections. The refined unit-cell parameters are $a = 10.9318(12)$, $c = 17.069(2)$ Å and $V = 1766.6(4)$ Å^3. The statistical tests on $|E|$ values and systematic absences indicated the space-group symmetry $P\bar{3}1c$. The crystal structure of coquimbite was refined using *Shelxl*-2018 (Sheldrick, 2015) starting from the atomic coordinates given by Demartin *et al.* (2010a). Taking into account the results of the electron microprobe analysis, the site scattering at the three metal sites was modelled using the following scattering curves, taken from the *International Tables for Crystallography* (Wilson, 1992): Al *vs.* Fe at the Al site; Fe at the Fe(1) and Fe(2) sites; and S at the S site. The scattering curve of O and H were used at all the O and H positions, respectively. Although the hydrogen coordinates have been given in previous studies (e.g. Demartin *et al.*, 2010a), their positions were sought in the difference-Fourier maps. Soft restraints were

Table 4. Selected bond distances (Å) in coquimbite.

Al–Ow(1)	1.8880(13) ×6	S–O(2)	1.4571(14)
		S–O(1)	1.4632(14)
Fe(1)–O(4)	2.0011(13) ×6	S–O(4)	1.4881(13)
		S–O(3)	1.4898(14)
Fe(2)–O(3)	1.9739(14) ×3	<S–O>	1.4746
Fe(2)–Ow(3)	2.0019(15) ×3		
<Fe(2)–O>	1.9879		

Table 5. Hydrogen-bond lengths (*d* in Å) and angles (in °) for coquimbite.

D–H···*A*	*d*(*D*–H)	*d*(H···*A*)	*d*(*D*···*A*)	∠*DHA*
Ow(1)–H(11)···O(2)	0.90(19)	1.82(2)	2.706(2)	170(4)
Ow(1)–H(12)···O(1)	0.93(18)	1.734(19)	2.6549(19)	173(3)
Ow(2)–H(21)···O(2)	0.91(18)	1.90(2)	2.747(2)	155(3)
Ow(2)–H(22)···Ow(2)	0.93(2)	1.84(3)	2.748(4)	165(7)
Ow(2)–H(23)···Ow(2)	0.92(2)	1.83(2)	2.735(3)	166(6)
Ow(3)–H(31)···O(1)	0.909(18)	1.757(19)	2.661(2)	173(3)
Ow(3)–H(32)···Ow(2)	0.926(18)	1.73(2)	2.643(2)	171(4)

D – donor; *A* – acceptor.

Table 6. Bond-valence sums (in valence units) for coquimbite.*

Site	Al	Fe(1)	Fe(2)	S	Σv_{anions}	H bonds	$\Sigma v_{anions\ (corr.)}$
O(1)				1.54	1.54	+0.25 +0.25	2.04
O(2)				1.57	1.57	+0.22 +0.20	1.99
O(3)			$0.56^{\times3\downarrow}$	1.44	2.00		2.00
O(4)		$0.52^{\times6\downarrow}$		1.44	1.96		1.96
Ow(1)	$0.54^{\times6\downarrow}$				0.54	−0.22 −0.25	0.07
Ow(2)					0.00	−0.20 +0.26	0.06
Ow(3)			$0.52^{\times3\downarrow}$		0.52	−0.25 −0.26	0.01
$\Sigma v_{cations}$	3.24	3.12	3.24	5.99			

*The number of equivalent bonds involving anions are indicated by ×↓. Bond parameters after Brese and O'Keeffe (1991). The bond-valence sums at the anion sites were corrected taking into account O···O distances (see Table 5) and the relationship of Ferraris and Ivaldi (1988).

https://doi.org/10.1180/mgm.2020.15 Published online by Cambridge University Press

Table 7. Coquimbite and related minerals.

Mineral	Chemical formula	Space group	Unit-cell parameters (Å)	References
Coquimbite group				
Coquimbite	$AlFe_3(SO_4)_6(H_2O)_{12}\cdot 6H_2O$	$P\bar{3}1c$	$a = 10.9318(12)$, $c = 17.069(2)$	This work
Paracoquimbite	$Fe_4(SO_4)_6(H_2O)_{12}\cdot 6H_2O$	$R\bar{3}$	$a = 10.963(16)$, $c = 51.473(10)$	Yang and Giester (2018)
Unassigned mineral				
Aluminocoquimbite	$Al_2Fe_2(SO_4)_6(H_2O)_{12}\cdot 6H_2O$	$P\bar{3}1c$	$a = 10.707(7)$, $c = 17.308(11)$	Demartin *et al.* (2010b)

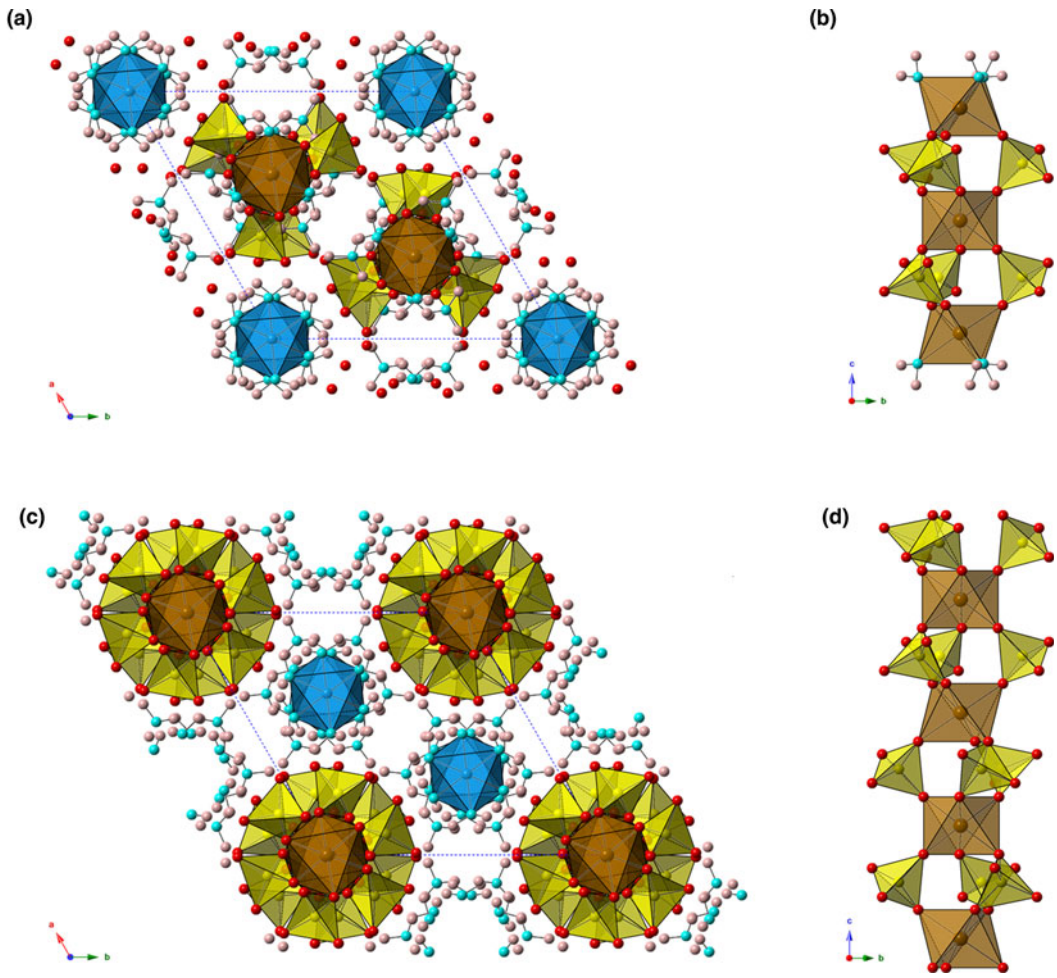

Fig. 5. The crystal structure of coquimbite, as seen down **c** (*a*). It is formed by finite clusters composed by Fe-centred octahedra and SO_4 groups (*b*). Aluminocoquimbite shows a different topology (*c*) and its crystal structure is characterised by infinite columns, running along **c**, formed by Fe-centred octahedra and SO_4 groups (*d*). Iron-, Al-, and S-centred polyhedra are shown in brown, blue, and yellow, respectively. Hydrogen atoms are shown as pink spheres, whereas O atoms are shown as red or, if belonging to H_2O groups, as light blue spheres.

used in order to avoid O–H distances that were too short. An anisotropic model for all the atom positions (except for H atoms) converged to 0.0219 for 1307 reflections with $F_o > 4\sigma(F_o)$ and 110 refined parameters. Details of data collection and refinement are given in Table 2. Atomic coordinates and isotropic or equivalent isotropic displacement parameters for coquimbite are given in Table 3, and selected bond distances are given in Table 4. In agreement with the previous studies, the crystal structure of coquimbite is characterised by the occurrence of clusters of composition $[FeFe_2(SO_4)_6(H_2O)_6]^{3-}$ and by isolated $[Al(H_2O)_6]^{3+}$ octahedra. Six symmetry-related H_2O groups, held in the structure through H-bonding only, are arranged in a cyclohexane-like chair conformation (e.g. Demartin *et al.*, 2010a). Table 5 reports the geometrical features of the H-bonds, whereas Table 6 gives the bond-valence balance. The crystallographic information files have been deposited with the Principal Editor of *Mineralogical Magazine* and are available as Supplementary material (see below).

Discussion and conclusion

On the basis of the examination of previous mineralogical investigations as well as of new crystal-chemical data, coquimbite has been redefined as $AlFe_3(SO_4)_6(H_2O)_{12}\cdot 6H_2O$ ($Z = 2$). Neotype material can be considered the sample studied by Fang and Robinson (1970) from the Tierra Amarilla (the original type locality described by Rose, 1833) and stored in the National Museum of Natural History (Smithsonian Institution, USA; catalogue number 12548). The sample from Monte Arsiccio studied in

https://doi.org/10.1180/mgm.2020.15 Published online by Cambridge University Press

this work, embedded in epoxy and polished, is kept in the mineralogical collection of the Museo di Storia Naturale of the University of Pisa, Italy, under catalogue number 19914.

In order to be compared with coquimbite, the chemical formulae of paracoquimbite and aluminocoquimbite are given as $Fe_4(SO_4)_6(H_2O)_{12}\cdot 6H_2O$ ($Z = 6$) and $Al_2Fe_2(SO_4)_6(H_2O)_{12}\cdot 6H_2O$ ($Z = 2$), respectively (Table 7).

Coquimbite and paracoquimbite are characterised by homeotypic structures, being formed by the same $[FeFe_2(SO_4)_6(H_2O)_6]^{3-}$ clusters and isolated $Me^{3+}(H_2O)_6$ (Me = Al, Fe) octahedra (Fig. 5*a*,*b*). Consequently, they fit with the definition of mineral group given by Mills *et al.* (2009): "*A mineral group consists of two or more minerals with the same or essentially the same structure, and composed of chemically similar elements*". They form the 'coquimbite group'. Aluminocoquimbite is characterised by a different topology, with infinite heteropolyhedral columns running along [001] (Fig. 5*c*, *d*), similar to those observed in ferrinatrite, $Na_3(H_2O)_3[Fe(SO_4)_3]$ (Ventruti *et al.*, 2019; Yang and Giester, 2019). Consequently, aluminocoquimbite does not belong to the coquimbite group.

As coquimbite is an Al-bearing compound, whereas paracoquimbite is Al-free, it is likely that the presence of Al stabilises the coquimbite structure, whereas its absence favours the crystallisation of paracoquimbite, in agreement with Majzlan *et al.* (2010). Higher Al content promotes the crystallisation of aluminocoquimbite. However, Giester and Miletich (1995) were able to synthesise $Fe_4(SeO_4)_3(H_2O)_{12}\cdot 6H_2O$ with the coquimbite structure. Therefore, should the natural sulfate analogue of synthetic $Fe_4(SeO_4)_3(H_2O)_{12}\cdot 6H_2O$ be discovered, the name 'ferricoquimbite' is suggested.

Acknowledgements. Mario Bianchini and Massimo D'Orazio are thanked for providing us with the specimens of coquimbite from the Monte Arsiccio mine. CB acknowledges financial support from the University of Pisa through the project P.R.A. 2018–2019 "Georisorse e Ambiente" (Grant No. PRA_2018_41). Peter Leverett, two anonymous reviewers, and the Associate Editor František Laufek are acknowledged for their comments and corrections.

Supplementary material. To view supplementary material for this article, please visit https://doi.org/10.1180/mgm.2020.15

References

Ackermann S., Armbruster T., Lazic B., Doyle S., Grevel K.-D. and Majzlan J. (2009) Thermodynamic and crystallographic properties of kornelite ($Fe_2(SO_4)_3\cdot\sim 7.75H_2O$) and paracoquimbite ($Fe_2(SO_4)_3\cdot 9H_2O$). *American Mineralogist*, **94**, 1620–1628.

Arzruni A. (1879) Ueber den Coquimbit. *Zeitschrift für Kristallographie, Mineralogie und Petrographie*, **3**, 516–524.

Bandy M.C. (1938) Mineralogy of three sulphate deposits of northern Chile. *American Mineralogist*, **23**, 669–760.

Biagioni C., Bonaccorsi E. and Orlandi P. (2011) Volaschioite, $Fe_4^{3+}(SO_4)O_2(OH)_6\cdot 2H_2O$, a new mineral species from Fornovolasco, Apuan Alps, Tuscany, Italy. *The Canadian Mineralogist*, **49**, 605–614.

Biagioni C., Bindi L., Mauro D. and Hålenius U. (2019) Crystal chemistry of sulfates from the Apuan Alps (Tuscany, Italy). V. Scordariite, $K_8(Fe_{0.67}^{3+}\square_{0.33})[Fe_3^{3+}O(SO_4)_6(H_2O)_3]_2(H_2O)_{11}$: a new metavoltine-related mineral. *Minerals*, **9**, 702.

Breithaupt J.F.A. (1841) Coquimbites ferricus kürzer Coquimbit. Pp. 100 in: *Vollständiges Handbuch der Mineralogie*. Volume **2**. Arnoldische Buchhandlung, Dresden and Leipzig, Germany.

Brese N.E. and O'Keeffe M. (1991) Bond-valence parameters for solids. *Acta Crystallographica*, **B47**, 192–197.

Bruker AXS Inc. (2016) *APEX* 3. Bruker Advanced X-ray Solutions, Madison, Wisconsin, USA.

Cesbron F. (1964) Contribution à la Minéralogie des sulfates de fer hydratés. *Bulletin de la Société Française de Mineralogie*, **87**, 125–143.

Collins H.F. (1923) On some crystallized sulphates from the province of Huelva, Spain. *Mineralogical Magazine*, **20**, 32–38.

Demartin F., Castellano C., Gramaccioli C.M. and Campostrini I. (2010a) Aluminum-for-iron substitution, hydrogen bonding, and a novel structure-type in coquimbite-like minerals. *The Canadian Mineralogist*, **48**, 323–333.

Demartin F., Castellano C., Gramaccioli C.M. and Campostrini I. (2010b) Aluminocoquimbite, $AlFe(SO_4)_3\cdot 9H_2O$, a new aluminum iron sulfate from Grotta dell'Allume, Vulcano, Aeolian Islands, Italy. *The Canadian Mineralogist*, **48**, 1465–1468.

Fanfani I., Nunzi A. and Zanazzi P.F. (1971) The crystal structure of butlerite. *American Mineralogist*, **56**, 751–757.

Fang J.H. and Robinson P.D. (1970) Crystal structures and mineral chemistry of hydrated ferric sulfates. I. The crystal structure of coquimbite. *American Mineralogist*, **55**, 1534–1540.

Fang J.H. and Robinson P.D. (1974) Polytypism in coquimbite and paracoquimbite. *Neues Jahrbuch für Mineralogie, Monatshefte*, **1974**, 89–91.

Fernandez-Martinez A., Timon V., Roman-Ross G., Cuello G.J., Daniels J.E. and Ayora C. (2010) The structure of schwertmannite, a nanocrystalline iron oxyhydroxysulfate. *American Mineralogist*, **95**, 1312–1322.

Ferraris G. and Ivaldi G. (1988) Bond valence vs bond length in O···O hydrogen bonds. *Acta Crystallographica*, **B44**, 341–344.

Frost R.L., Žigovečki Gobac Ž., López A., Xi Y., Scholz R., Lana C. and Fernandes Lima R.M. (2014) Characterization of the sulphate mineral coquimbite, a secondary iron sulphate from Javier Ortega mine, Lucanas Province, Peru – Using infrared, Raman spectroscopy and thermogravimetry. *Journal of Molecular Structure*, **1063**, 251–258.

Giacovazzo C., Menchetti S. and Scordari F. (1970) The crystal structure of coquimbite. *Atti della Accademia Nazionale dei Lincei, Rendiconti della Classe di Scienze Fisiche, Matematiche e Naturali*, **49**, 129–140.

Giester G. and Miletich R. (1995) Crystal structure and thermal decomposition of the coquimbite-type compound $Fe_2(SeO_4)_3\cdot 9H_2O$. *Neues Jahrbuch für Mineralogie, Monatshefte*, **1995**, 211–223.

Jambor J.L., Nordstrom D.K. and Alpers C.N. (2000) Metal-sulfate salts from sulfide mineral oxidation. Pp. 303–350 in: *Sulfate Minerals: Crystallography, Geochemistry, and Environmental Significance* (C.N. Alpers, J.L. Jambor, and D.K Nordstrom, editors). Reviews in Mineralogy & Geochemistry, **40**. Mineralogical Society of America and the Geochemical Society, Washington, DC.

Lausen C. (1928) Hydrous sulphates formed under fumerolic conditions at the United Verde mine. *American Mineralogist*, **13**, 203–229.

Linck G. (1889) Beitrag zur Kenntniss der Sulfate von Tierra amarilla bei Copiapó in Chile. *Zeitschrift für Kristallographie und Mineralogie*, **15**, 1–28.

Majzlan J. and Kiefer B. (2006) An X-ray and neutron-diffraction study of synthetic ferricopiapite, $Fe_{14/3}(SO_4)_6(OD,OH)_2(D_2O,H_2O)_{20}$, and ab initio calculations on the structure of magnesiocopiapite, $MgFe_4(SO_4)_6(OH)_2(H_2O)_{20}$. *The Canadian Mineralogist*, **44**, 1227–1237.

Majzlan J., Botez C. and Stephens P.W. (2005) The crystal structures of synthetic $Fe_2(SO_4)_3(H_2O)_5$ and the type specimen of lausenite. *American Mineralogist*, **90**, 411–416.

Majzlan J., Navrotsky A., McCleskey R.B. and Alpers C.N. (2006) Thermodynamic properties and crystal structure refinement of ferricopiapite, coquimbite, rhomboclase, and $Fe_2(SO_4)_3(H_2O)_5$. *European Journal of Mineralogy*, **18**, 175–186.

Majzlan J., Dordević T., Kolitsch U. and Schefer J. (2010) Hydrogen bonding in coquimbite, nominally $Fe_2(SO_4)_3\cdot 9H_2O$, and the relationship between coquimbite and paracoquimbite. *Mineralogy and Petrology*, **100**, 241–248.

Majzlan J., Dachs E., Benisek A., Plášil J. and Sejkora J. (2018) Thermodynamics, crystal chemistry and structural complexity of the $Fe(SO_4)(OH)(H_2O)_x$ phases: $Fe(SO_4)(OH)$, metahohmannite, butlerite, parabutlerite, amarantite, hohmannite, and fibroferrite. *European Journal of Mineralogy*, **30**, 259–275.

Mills S.J., Hatert F., Nickel E.H. and Ferraris G. (2009) The standardisation of mineral group hierarchies: application to recent nomenclature proposals. *European Journal of Mineralogy*, **21**, 1073–1080.

Miyawaki R., Hatert F., Pasero M. and Mills S.J. (2019) New minerals and nomenclature modifications approved in 2019. IMA Commission on New

Minerals, Nomenclature and Classification (CNMNC), Newsletter 52. *Mineralogical Magazine*, **83**, 887–893.

Palache C., Berman H. and Frondel C. (1951) *The System of Mineralogy of James Dwight Dana and Edward Salisbury Dana, Yale University 1837–1892.* 7th edition, Vol. **II**. John Wiley and Sons Inc., New York [pp. 532–534].

Pasero, M. (2019) *The New IMA List of Minerals*. http://cnmnc.main.jp/ [accessed May 2019].

Peterson R.C., Valyashko E. and Wang R. (2009) The atomic structure of $(H_3O)Fe^{3+}(SO_4)_2$ and rhomboclase, $(H_5O_2)Fe^{3+}(SO_4)_2{\cdot}2H_2O$. *The Canadian Mineralogist*, **47**, 625–634.

Plášil J., Škoda R., Fejfarová K., Čejka J., Kasatkin A.V., Dušek M., Talla D., Lapčák L., Machovič V. and Dini M. (2014) Hydroniumjarosite, $(H_3O)^+Fe_3(SO_4)_2(OH)_6$, from Cerros Pintados, Chile: Single-crystal X-ray diffraction and vibrational spectroscopic study. *Mineralogical Magazine*, **78**, 535–547.

Robinson P.D. and Fang J.H. (1971) Crystal structures and mineral chemistry of hydrated ferric sulphates: II. The crystal structure of paracoquimbite. *American Mineralogist*, **56**, 1567–1572.

Robinson P.D. and Fang J.H. (1973) Crystal structures and mineral chemistry of hydrated ferric sulphates. III. The crystal structure of kornelite. *American Mineralogist*, **58**, 535–539.

Rose H. (1833) Ueber einige in Südamerika vorkommende Eisenoxydsalze. *Annalen der Physik und Chemie*, **27**, 309–319.

Scharizer R. (1927) XXI. Beitrage zur Kenntnis der chemischen Konstitution und der Genese der natürlichen Ferrisulfate. *Zeitschrift für Kristallographie und Mineralogie*, **65**, 335–360.

Scordari F., Ventruti G. and Gualtieri A. (2004) The structure of metahohmannite, $Fe_2^{3+}[O(SO_4)_2]{\cdot}4H_2O$, by in situ synchrotron powder diffraction. *American Mineralogist*, **89**, 365–370.

Sheldrick G.M. (2015) Crystal structure refinement with SHELXL. *Acta Crystallographica*, **C71**, 3–8.

Susse P. (1968) The crystal structure of amarantite, $Fe_2(SO_4)_2O{\cdot}7H_2O$. *Zeitschrift für Kristallographie*, **127**, 261–275.

Thomas J.N., Robinson P.D. and Fang J.H. (1974) Crystal structures and mineral chemistry of hydrated ferric sulfates. IV. The crystal structure of quenstedtite. *American Mineralogist*, **59**, 582–586.

Ungemach H. (1933) Sur quelques minéraux nouveaux. *Comptes Rendus de l'Académie des Sciences de Paris*, **197**, 1132–1134.

Ungemach H. (1935) Sur certains minéraux sulfatés du Chili. *Bulletin de la Société Française de Mineralogie*, **58**, 97–221.

Ventruti G., Della Ventura G., Orlando R. and Scordari F. (2015) Structure refinement, hydrogen-bond system and vibrational spectroscopy of hohmannite, $Fe_2^{3+}[O(SO_4)_2]{\cdot}8H_2O$. *Mineralogical Magazine*, **79**, 11–24.

Ventruti G., Della Ventura G., Bellatreccia F., Lacalamita M. and Schingaro E. (2016) Hydrogen bond system and vibrational spectroscopy of the iron sulfate fibroferrite, $Fe(OH)SO_4{\cdot}5H_2O$. *European Journal of Mineralogy*, **28**, 943–952.

Ventruti G., Della Ventura G., Lacalamita M., Sbroscia M., Sodo A., Plaisier J.R., Cinque G. and Schingaro E. (2019) Crystal-chemistry and vibrational spectroscopy of ferrinatrite, $Na_3[Fe(SO_4)_3]{\cdot}3H_2O$, and its high-temperature decomposition. *Physics and Chemistry of Minerals*, **46**, 119–131.

Wilson A.J.C. (1992) *International Tables for Crystallography. Volume C*. Kluwer, Dordrecht, Germany.

Yang Z. and Giester G. (2018) Structure refinements of coquimbite and paracoquimbite from the Hongshan Cu-Au deposit, NW China. *European Journal of Mineralogy*, **30**, 849–858.

Yang Z. and Giester G. (2019) Structure refinement and hydrogen bonding of ferrinatrite, $Na_3Fe(SO_4)_3{\cdot}3H_2O$. *Mineralogy and Petrology*, **113**, 555–562.